http://eprints.gla.ac.uk/32455/

Deposited on: 18th July 2012

Three-dimensional parallel holographic micropatterning using a spatial light modulator

Nathan J. Jenness[1], Kurt D. Wulff[1], Matthew S. Johannes[1],
Miles J. Padgett[3], Daniel G. Cole[2], and Robert L. Clark[1]

[1]*Center for Biologically Inspired Materials and Material Systems*
Center for Biomolecular and Tissue Engineering
Duke University, Durham, NC, USA
[2]*Department of Mechanical Engineering and Materials Science*
University of Pittsburgh, Pittsburgh, PA, USA
[3]*Department of Physics and Astronomy*
University of Glasgow, Glasgow, Scotland, UK

nathan.jenness@duke.edu

Abstract: We present a micropatterning method for the automatic transfer and arbitrary positioning of computer-generated three-dimensional structures within a substrate. The Gerchberg-Saxton algorithm and an electrically addressed spatial light modulator (SLM) are used to create and display phase holograms, respectively. A holographic approach to light manipulation enables arbitrary and efficient parallel photo-patterning. Multiple pyramidal microstructures were created simultaneously in a photosensitive adhesive. A scanning electron microscope was used to confirm successful replication of the desired microscale structures.

References and links

1. W. H. Zhou, S. M. Kuebler, K. L. Braun, T. Y. Yu, J. K. Cammack, C. K. Ober, J. W. Perry, and S. R. Marder, "An efficient two-photon-generated photoacid applied to positive-tone 3D microfabrication," Science **296,** 1106-1109 (2002).
2. S. Kawata, H. B. Sun, T. Tanaka, and K. Takada, "Finer features for functional microdevices - Micromachines can be created with higher resolution using two-photon absorption," Nature **412,** 697698 (2001).
3. B. H. Cumpston, S. P. Ananthavel, S. Barlow, D. L. Dyer, J. E. Ehrlich, L. L. Erskine, A. A. Heikal, S. M. Kuebler, I. Y. S. Lee, D. McCord-Maughon, J. Q. Qin, H. Rockel, M. Rumi, X. L. Wu, S. R. Marder, and J. W. Perry, "Twophoton polymerization initiators for three-dimensional optical data storage and microfabrication," Nature **398,** 5154 (1999).
4. C. B. Arnold and A. Pique, "Laser Direct-Write Processing," MRS Bulletin **32,** 915 (2007).
5. H. B. Yin, T. Brown, J. S. Wilkinson, R. W. Eason, and T. Melvin, "Submicron patterning of DNA oligonucleotides on silicon," Nucleic Acids Research **32,** (2004).
6. A. Lachish-Zalait, D. Zbaida, E. Klein, and M. Elbaum, "Direct surface patterning from solutions: Localized microchemistry using a focused laser," Adv. Funct. Mater. **11,** 218223 (2001).
7. R. T. Hill and J. B. Shear, "Enzyme-nanoparticle functionalization of three-dimensional protein scaffolds," Anal. Chem. **78,** 70227026 (2006).
8. B. Kaehr, N. Ertas, R. Nielson, R. Allen, R. T. Hill, M. Plenert, and J. B. Shear, "Direct-write fabrication of functional protein matrixes using a low-cost Q-switched laser," Anal. Chem. **78,** 31983202 (2006).
9. K. Itoga, J. Kobayashi, M. Yamato, A. Kikuchi, and T. Okano, "Maskless liquid-crystal-display projection photolithography for improved design flexibility of cellular micropatterns," Biomaterials **27,** 30053009 (2006).
10. T. Kondo, S. Juodkazis, V. Mizeikis, H. Misawa, and S. Matsuo, "Holographic lithography of periodic two- and three-dimensional microstructures in photoresist SU-8," Opt. Express **14,** 79437953 (2006).
11. S. Hasegawa, Y. Hayasaki, and N. Nishida, "Holographic femtosecond laser processing with multiplexed phase Fresnel lenses," Opt. Lett. **31,** 17051707 (2006).

12. Y. Kuroiwa, N. Takeshima, Y. Narita, S. Tanaka, and K. Hirao, "Arbitrary micropatterning method in femtosecond laser microprocessing using diffractive optical elements," Opt. Express **12,** 19081915 (2004).
13. N. J. Jenness, K. D. Wulff, M. S. Johannes, D. G. Cole, and R. L. Clark, "Dynamic Maskless Holographic Lithography," Proceedings of ASME IDETC/CIE 2007 Micro- and Nanosystems (2007).
14. J. E. Curtis, B. A. Koss, and D. G. Grier, "Dynamic holographic optical tweezers," Opt. Commun. **207,** 169175 (2002).
15. J. Leach, K. Wulff, G. Sinclair, P. Jordan, J. Courtial, L. Thomson, G. Gibson, K. Karunwi, J. Cooper, Z. J. Laczik, and M. Padgett, "Interactive approach to optical tweezers control," Appl. Opt. **45,** 897903 (2006).
16. M. S. Johannes, J. F. Kuniholm, D. G. Cole, and R. L. Clark, "Automated CAD/CAM-based nanolithography using a custom atomic force microscope," IEEE Transactions on Automation Science and Engineering **3,** 236239 (2006).
17. J. Liesener, M. Reicherter, T. Haist, and H. J. Tiziani, "Multi-functional optical tweezers using computer-generated holograms," Opt. Commun. **185,** 7782 (2000).
18. R.W. Gerchberg andW. O. Saxton, "A practical algorithm for the determination of phase image and diffraction plane pictures," Optik **35,** 237248 (1972).
19. M. A. Seldowitz, J. P. Allebach, and D. W. Sweeney, "Synthesis of Digital Holograms by Direct Binary Search," Appl. Opt. **26,** 27882798 (1987).
20. T. Tanaka, H. B. Sun, and S. Kawata, "Rapid sub-diffraction-limit laser micro/nanoprocessing in a threshold material system," Appl. Phys. Lett. **80,** 312314 (2002).
21. W. H. Teh, U. Durig, G. Salis, R. Harbers, U. Drechsler, R. F. Mahrt, C. G. Smith, and H. J. Guntherodt, "SU-8 for real three-dimensional subdiffraction-limit two-photon microfabrication," Appl. Phys. Lett. **84,** 40954097 (2004).

1. Introduction

The ability to localize laser power to predetermined areas through the use of laser direct-write (LDW) lithography is a well accepted method for maskless microfabrication [1, 2]. During this process, three-dimensional (3D) structures are transferred by serially scanning a highly focused laser beam within a photosensitive material. The localized photoexcitation that results from exposure to the beam crosslinks targeted regions and reduces solubility. The desired structure is then obtained by dissolving away the remaining unexposed material [3, 4]. Direct-write technology traditionally applied to the semiconductor industry has recently been used in new applications including the fabrication of DNA oligonucleotide sensors on silicon [5] and the production of localized chemical reactivity on target substrates [6, 7, 8]. LDW is an attractive lithographic technique because it eliminates the need to construct and align masks while offering non-contact pattern transfer for chemically and mechanically sensitive substrates. The process is strictly serial, however, which can result in fabrication times of several minutes to hours for a single structure. This effectively precludes the direct mass production of structures using LDW processes.

In order to improve processing throughput and reduce costs, several parallel laser-based lithographic techniques are under development. Diffractive optical elements (DOE) have been used to directly project and transfer arbitrary patterns onto glass and biological substrates [9]. DOEs offer excellent control over array and image generation; however, they can dilute laser power and require multi-axis stages for 3D structure creation. In order to maximize power delivery, holographic techniques such as multibeam interference and multiplexed phase Fresnel lenses (MPFL) have been used for microfabrication [10, 11, 12]. The advantage of multibeam interference is the ability to pattern large-scale areas; however, the system requires complex alignment, and it proves difficult to control the shape and position of the interference area. The MPFL method provides an efficient method for directing light in three dimensions, but to date only simple ablation patterns have been produced on glass.

We seek to advance current micro/nano patterning by integrating holographic techniques with photolithography to create a rapidly reconfigurable, maskless, parallel, and mechanically static 3D patterning tool. This is accomplished by expanding previously described two-dimensional dynamic maskless holographic lithography (DMHL) [13] to a third dimension. The use of a spatial light modulator (SLM) enables the instantaneous display of various phase holograms [14, 15]. The benefit of a holographic approach lies in the freedom to direct laser light to any point or in any pattern without the use of a mechanical stage or photomask. A second thrust of this research

is the creation of a user-accessible and customizable instrument. All design and control aspects are performed in common software packages, namely SolidWorks and MATLAB, facilitating the operation and use of the instrument. The individual user has control over the entire set of system parameters. The method presented, capable of generating 3D micro/nanoscale structures in a re-configurable and user-friendly process, will push the state-of-the-art concerning the industrial and research manufacturing validity of photolithography.

2. Optical setup

The holographic patterning system (Fig. 1.) is built around a Zeiss Axiovert 200 inverted microscope (with a NA 1.4, 100x Zeiss Plan-Neofluar oil-immersion objective) and a Melles Griot ND:YAG continuous wave 532 nm laser. The phase holograms generated for each structure are displayed on a Holoeye LC-R 2500 electrically addressed SLM. The laser beam is polarized by a 1/2 waveplate before being expanded and collimated to slightly overfill the SLM display. Proper polarization ensures maximum energy transfer during phase modulation, while a slight overfill ensures the beam is incident upon the entire SLM display. Using a series of lenses and mirrors the phase modulated light from the SLM is directed through the microscope objective illuminating the focal plane. Only the first diffraction order is used for patterning; therefore, unwanted diffraction orders created by the SLM are removed by spatial filtering. A dichroic beam splitter enables real-time charge-coupled device (CCD) monitoring of the sample surface. The entire system is mounted on a vibration isolation table to minimize disturbances.
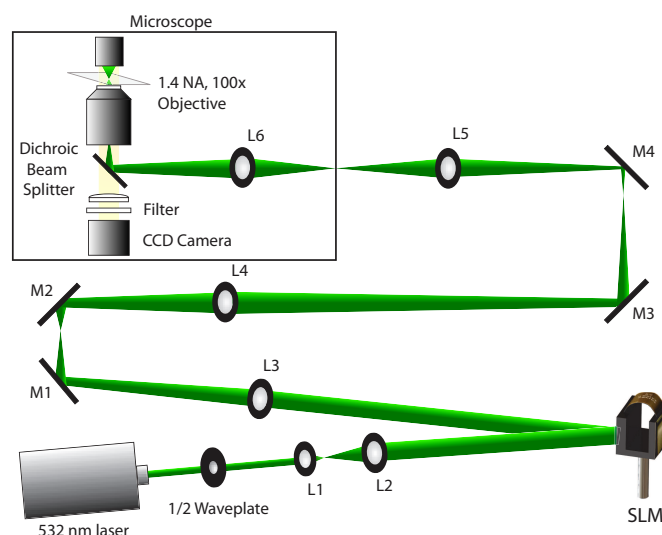

Fig. 1. Schematic diagram of the holographic system. The SLM plane is imaged onto the pupil plane of the microscope objective using lenses (L) and mirrors (M).

3. Manufacturing procedure

The manufacturing process can be broken down into two major components: CAD-based structure design and hologram generation. Desired structures are generated in the computer aided drafting (CAD) software package SolidWorks and translated into phase holograms using MATLAB. The use of CAD software enables the virtual design, manipulation, and preview of complex structures. Once structures are designed and reviewed in SolidWorks (Fig. 2(a).), they are saved as stereolithography (STL) files. The STL files are converted into G-code using a standard STL to G-code converter. G-code is a programming language/interface typically used in macroscale computer nu-
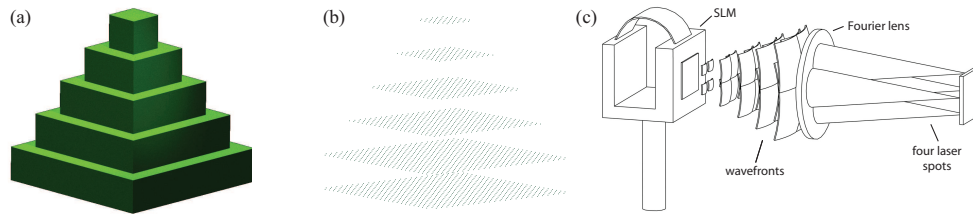
Fig. 2. (a) CAD representation of a square pyramid. (b) MATLAB plot of CAD structure discretized into points by layer. (c) Schematic of the single beam conversion into multiple focal points for parallel processing.

meric control (CNC) milling machines, however, it has been shown to effectively control motion at the nanoscale [16]. As shown in Fig. 2(b), a MATLAB script reads and converts the G-code into Cartesian coordinates. The coordinates are sorted by axial (z) value and then lateral (x,y) values to produce an ordered 3D laser path for layer-by-layer structure fabrication. Using this path, a single beam is divided into multiple focused laser spots to simultaneously write several structures.

Several algorithms are available to calculate the phase holograms necessary for the formation of multiple focused laser spots. These algorithms include gratings and lenses [17], Gerchberg-Saxton [18], and direct binary search [19]. The Gerchberg-Saxton algorithm was chosen to compute phase holograms in this system due to a combination of calculation speed and accuracy. This iterative Fourier-transform-based algorithm calculates the phase required in the hologram plane to produce a predefined intensity distribution in the focal plane. After completing several iterations the algorithm converges producing the desired phase, ϕ_{holo} [15, 18]. This hologram may be further modified to create lateral and axial shifts in the image plane.

In order to envision holographic lateral and axial shifts it is convenient to consider as an example, a single point. A beam with planar phase fronts at the hologram plane corresponds to a single focused point in the image space. It is simple to move this point around by altering the phase at the hologram plane. For example as shown in Fig. 3(a), a phase hologram that has an inclined phase front/grating will produce a point in the image plane displaced laterally proportional to the magnitude of the grating [15]. This concept is not exclusive to a single point and may be applied to entire images. The phase required to produce a lateral shift (Δx, Δy) is calculated by

$$\phi_{\text{grating}}(x_{\text{holo}}, y_{\text{holo}}) = 2\pi(\Delta x x_{\text{holo}} + \Delta y y_{\text{holo}}), \tag{1}$$

where x_{holo} and y_{holo} are components of the complex field at the focal plane of the microscope objective. Figure 3(b) shows a phase-based lens may also be implemented to move the focal point or image axially within a substrate. The lens is composed of a series of concentric circles, which directs light in the same manner as a traditional physical lens. The phase-based lens changes the focal length of the entire system resulting in an axial displacement. The phase necessary to accomplish this movement is defined by

$$\phi_{\text{lens}}(x_{\text{holo}}, y_{\text{holo}}) = \frac{2\pi\Delta f}{\lambda f^2}(x_{\text{holo}}^2 + y_{\text{holo}}^2), \tag{2}$$

where f is the focal length, Δf is the desired change in focal length, and λ is the wavelength of light. The total phase, incorporating both the lateral shift and axial shift along with the image phase, may be calculated by

$$\phi_{\text{total}} = \mod(\phi_{\text{holo}} + \phi_{\text{grating}} + \phi_{\text{lens}}, 2\pi). \tag{3}$$

For 3D patterning, the use of several axial shifts enables the precise positioning of distinct structural features in several planes.
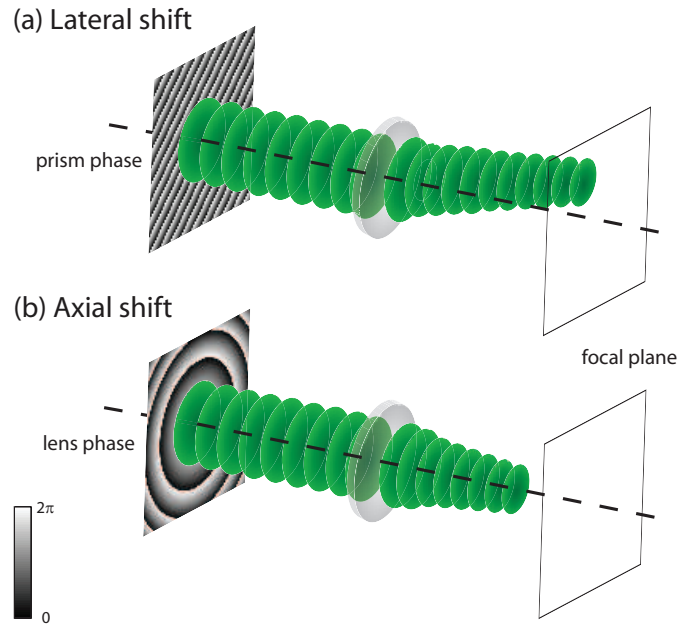
Fig. 3. Phase required for the (a) lateral positioning $\phi_{grating}$ and (b) axial positioning ϕ_{lens} of the individual points within a 3D structure.

This system offers user control over a few key parameters to produce desired feature characteristics. In addition to lateral and axial positioning, the parameters controlled include incident intensity and write speed. Potential substrates require varying doses of laser radiation to reach their respective patterning thresholds making power adaptability paramount [20, 21]. The laser source is adjustable from 0.0 - 2.7 W, however, exposure can be further modified by adjusting the frame rate of the holograms displayed to dictate the write speed.

4. Substrate selection and preparation

Norland NOA 63, an ultraviolet (UV) curing adhesive with optimum sensitivity in the 350-400 nm range, was the photopolymer selected for patterning. The sensitivity of the adhesive lies outside the wavelength of the laser (at 500-600 nm the material allows 99% transmission) permitting intensity-based threshold processing. In other words, the adhesive polymer will not crosslink/cure unless a minimum laser intensity is applied, resulting in 3D spatial specificity.

The following procedures were used to prepare each sample. The photopolymer was applied directly to the surface of a coverslip in the form of a droplet and allowed to expand to equilibrium. Pattern transfer was observed via the CCD camera in realtime as the sample was exposed to the SLM-modulated laser beam. After transfer had completed, non-crosslinked adhesive was removed by washing with pure methanol. Nitrogen was used to dry the sample after washing.

Both a standard scanning electron microscope (SEM) and environmental scanning electron microscope (ESEM) were used to view the resulting structures. The ESEM enables imaging of non-conductive substrates without requiring a metal coating, but provides lower resolution images. The standard SEM provides much higher resolution, but requires a metal coating to reduce spatial charging. The polymer structures were first imaged using the ESEM and then coated with 2 nm of chromium and 10 nm of gold using a metal evaporator for SEM imaging.
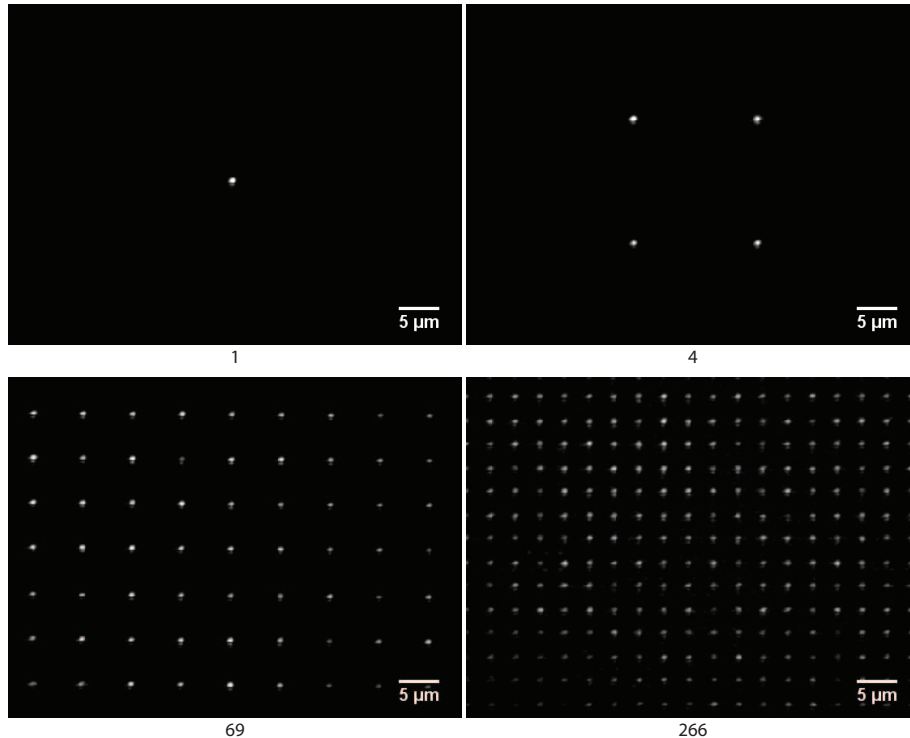
Fig. 4. Images from the CCD camera showing multiple focal points (number of points beneath each image) simultaneously displayed on a glass coverslip placed at the focal plane. Each image is of the entire 56 μm x 42 μm microscope objective field of view.

5. Results and discussion

As stated previously, the Gerchberg-Saxton algorithm is capable of creating several focal points simultaneously. Figure 4 demonstrates the ability to make from 1 to 266 points by phase modulating a single source beam. The number of focal points that could be used for patterning, however, was limited by source laser power, the diffraction efficiency of the SLM, and the field of view of the objective. Because the presented process relies on a threshold effect, a minimum intensity must be overcome at each focal point to cure the substrate. For the optical setup presented, four focal points could be derived from the source beam and used to create structures in the Norland adhesive. The diameter of each focal point was 0.9 μm (Fig. 4.). The height of a single cured layer of substrate revealed the depth of focus to be ~1.7 μm for the patterning system.

Using these parameters, four square pyramid structures were constructed in the CAD design environment. The pyramids were designed with side lengths of 10, 8, 6, 4, and 2 μm respectively. The prescribed heights of the pyramids were 10 μm. The four pyramids were written simultaneously using a single beam propagated from the proper series of phase holograms. The laser intensity was set to 2.0 W and the holograms writing the pyramids were displayed at 2 frames-per-second. The parameters were chosen based on past experience with this particular laser and material.

The pyramid structures required 2138 individual holograms for lithography resulting in a write time of 17.8 minutes. Screen shots and a video (Fig. 5 (Media 1).) were taken using the bright-field microscope to show the completion of each layer. We note the contrast change in the microscope images with the addition of each layer, an effect present due to the increased focal length resulting from building axially.
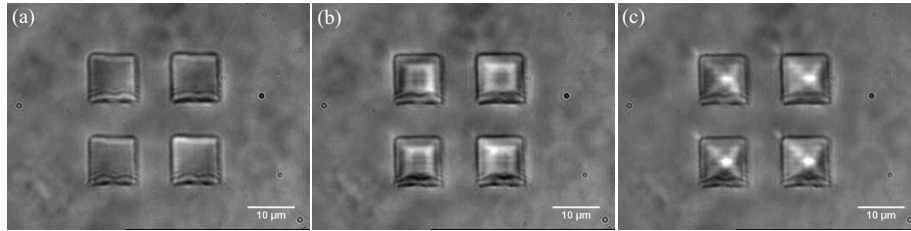
Fig. 5. Optical light microscope video of the fabrication process ([Media 1]) and images showing the completion of pyramidal layers (a) 2, (b) 4, and (c) 6 during processing.
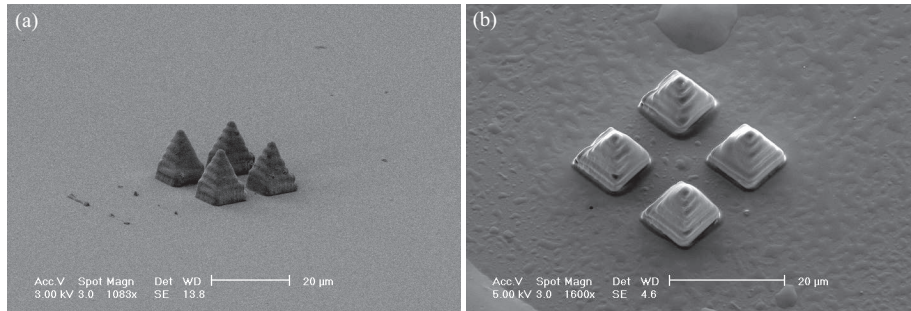

Fig. 6. SEM images of four simultaneously created square pyramids at angles of (a) 20° and (b) 45° from the surface.

Examining the results, the desired structures were successfully transferred to the Norland adhesive. The average side length and height of each pyramid was ∼10 μm, in agreement with CAD design. Comparison of the ESEM images and SEM images (Fig. 6.) provided verification that metal evaporation did not alter the final structures. The higher resolution SEM images highlight the distinct layers of the square pyramidal structures.

6. Conclusion

In this paper we have shown that spatial light modulators can be effective tools for arbitrary three dimensional laser-based parallel micro-manufacturing. Although there are many techniques currently implemented to produce 3D structures, limitations exist in the type of substrates, pattern intricacy, and parallel processing capabilities. The system presented combines the aforementioned characteristics while providing an user-accessible interface based in SolidWorks and MATLAB. Further optimization of DMHL will result in improved resolution and parallelization thereby expanding the capabilities and application of this technique.